Alexandria Engineering Journal (2016) xxx, xxx–xxx

HOSTED BY

Alexandria University

Alexandria Engineering Journal

www.elsevier.com/locate/aej
www.sciencedirect.com

ORIGINAL ARTICLE

Numerical investigation of combined buoyancy-thermocapillary convection and entropy generation in 3D cavity filled with Al_2O_3 nanofluid

Lioua Kolsi [a,b,*], Emtinene Lajnef [b], Walid Aich [a,c], Abdulaziz Alghamdi [a], Mohamed Ahmed Aichouni [a], Mohamed Naceur Borjini [b], Habib Ben Aissia [b]

[a] *College of Engineering, Mechanical Engineering Department, Haïl University, Haïl City, Saudi Arabia*
[b] *Unité de recherche de Métrologie et des Systèmes Énergétiques, École Nationale d'Ingénieurs, Monastir, University of Monastir, Tunisia*
[c] *Unité de Recherche Matériaux, Energie et Energies Renouvelables, Faculté des Sciences de Gafsa, University of Gafsa, Tunisia*

Received 26 January 2016; revised 21 May 2016; accepted 17 September 2016

KEYWORDS

Buoyancy-thermocapillary;
Nanofluids;
3D;
Entropy generation

Abstract Heat transfer, fluid flow and entropy generation due to combined buoyancy and thermocapillary forces in a 3D differentially heated enclosure containing Al_2O_3 nanofluid are carried out for different Marangoni numbers and different nanoparticles concentrations. The vector potential-vorticity formalism and the finite volume method are used respectively to formulate and to solve the governing equations and calculations were performed for Marangoni number from -10^3 to 10^3, volume fraction of nanoparticles from 0 to 0.2 and for a fixed Rayleigh number at 10^5. An intensification of the flow and an increase in heat transfer and of total entropy generation occur with the increase in nanoparticles volume fraction for all Marangoni numbers.

1. Introduction

The combined thermocapillary-natural convection is important for understanding many engineering applications and transport processes. The applications of this transport phenomenon, are crystal growth, solar energy, cooling of electronical devices, glass manufacturing, some chemical processing and building heating and ventilation. Fluids used in these applications such as water and mineral oils have restricted designers, because of their low thermal conductivity. Thus, nanofluids were developed to improve the heat exchange performances. Nanofluids are dilute liquid suspensions of nanoparticles with at least one critical dimension smaller than (100 nm) suspended stably and uniformly in a base liquid. The use of nanoparticles having high thermal conductivity produces a high thermal conductivity nanofluid. Many models have been proposed, focusing mainly on parameters such as geometry of nanoparticles, Brownian effects, temperature and interaction between nanoparticles and the base fluid. The first model was proposed by Maxwell [1] showing that

* Corresponding author at: College of Engineering, Mechanical Engineering Department, Haïl University, Haïl City, Saudi Arabia.
E-mail address: lioua_enim@yahoo.fr (L. Kolsi).
Peer review under responsibility of Faculty of Engineering, Alexandria University.

http://dx.doi.org/10.1016/j.aej.2016.09.005
1110-0168

Nomenclature

Be	Bejan number
C_p	specific heat at constant pressure (J/kg K)
g	gravitational acceleration (m/s^2)
k	thermal conductivity (W/m K)
l	enclosure width (m)
Ma	Marangoni Number
n	unit vector normal to the wall.
N_s	dimensionless local generated entropy
Nu	local Nusselt number
Pr	Prandtl number
Ra	Rayleigh number
S'_{gen}	generated entropy (kJ/kg K)
t	dimensionless time ($t'.\alpha/l^2$)
T	dimensionless temperature $[(T' - T'_c)/(T'_h - T'_c)]$
T'_c	cold temperature (K)
T'_h	hot temperature (K)
T_o	bulk temperature $[T_o = (T'_c + T'_h)/2]$ (K)
$\vec{V}$	dimensionless velocity vector ($\vec{V}' \cdot l/\alpha$)
x, y, z	dimensionless Cartesian coordinates ($x'/l, y'/l, z'/l$)

Greek symbols

α	thermal diffusivity (m^2/s)
β	thermal expansion coefficient (1/K)
ρ	density (kg/m^3)
μ	dynamic viscosity (kg/m s)
ν	kinematic viscosity (m^2/s)
φ	nanoparticle or solid volume fraction
φ_e	irreversibility coefficient
$\vec{\psi}$	dimensionless vector potential ($\vec{\psi}'/\alpha$)
$\vec{\omega}$	dimensionless vorticity ($\vec{\omega}' \cdot \alpha/l^2$)
ΔT	dimensionless temperature difference

Subscripts

av	average
x, y, z	Cartesian coordinates
fr	friction
f	fluid
max	maximum
nf	nanofluid
s	solid
th	thermal
tot	total

Superscript

$'$	dimensional variable

thermal conductivity of nanofluid increases with increase in volume fraction of solid nanoparticles.

Straub et al. [2] studied numerically the enhancement of heat transfer by thermocapillary convection around bubbles. They observed that oscillatory flow behavior occurs for higher Marangoni numbers. Behnia et al. [3] solved the problem of combined buoyancy and thermocapillary convection in an upright cube with a top free surface while all other walls are considered to be solid and impermeable. Equations were written using the velocity-vorticity formulation and solved using approximations of the finite difference method. Peng et al. [4] performed a work to understand the characteristics of thermocapillary-buoyancy flow of unsteady three-dimensional flow of 0.65cSt silicone oil with $Pr = 6.7$ in an annular pool with different depths. An example of application is presented by Lee et al. [5] on combined thermocapillary and natural convection in rectangular containers. They heated the fluid by a thin wire placed along the free surface. They observed that the flow becomes oscillatory when the convection becomes sufficiently large. Babu and Korpela [6] solved the three-dimensional thermocapillary convection in a cubical cavity. They used finite difference procedure to solve governing equations. Results were presented for low Marangoni numbers. Oztop et al. [7] studied the combined buoyancy-thermocapillary driven convection for different values of Marangoni and Rayleigh numbers inside a cubic cavity. They mentioned that entropy generation due to heat transfer and fluid friction increases with increase in Rayleigh and Marangoni numbers and the flow structure is affected for both negative and positive values of Marangoni number. Heat transfer enhancement in a two-dimensional enclosure utilizing nanofluids was investigated numerically by Khanafer et al. [8]. The results illustrate that the nanofluid heat transfer rate increases with an increase in the nanoparticles volume fraction. The presence of nanoparticles in the fluid is found to alter the structure of the fluid flow. These main findings are obtained in various other configurations considered by Oztop and Abu-Nada [9], Mahmoudi et al. [10,11], Mahmoodi [12], Mahmoudi and Sebdan [13], Nasrin, and Alim [14], Hassan [15] and Fontes et al. [16]. Recently Kolsi et al. [17] investigated numerically natural convection and entropy generation inside a three-dimensional cubical enclosure filled with water-Al_2O_3 nanofluid. The second law of thermodynamics was applied to predict entropy generation rate. The results explain that average Nusselt number and total entropy generation increase when the nanoparticles volume fraction and Rayleigh number increase.

The only work found on combined thermocapillary buoyancy convection of nanofluids is that of Aminfar et al. [21]. They presented a numerical investigation of thermocapillary and buoyancy driven convection of silicone oil based nanofluid with Al_2O_3 nanoparticles in a floating zone. The results indicated that, in the absence of gravity, when thermocapillary effect is the only source of convection, increasing the volume fraction of nanoparticles causes an increase in nanofluid Marangoni number, heat transfer coefficient and Nusselt number. In the presence of gravity, increasing the volume fraction of nanoparticles decreases both the thermocapillary and buoyancy driven heat transfer coefficients and as a result the Nusselt number.

Therefore, it is seen from the above literature review that, there is no research up to date dealing with the combined thermocapillary-buoyancy convection and entropy generation in a cubical cavity filled with a nanofluid. This represents the

Please cite this article in press as: L. Kolsi et al., Numerical investigation of combined buoyancy-thermocapillary convection and entropy generation in 3D cavity filled with Al_2O_3 nanofluid, Alexandria Eng. J. (2016), http://dx.doi.org/10.1016/j.aej.2016.09.005

first original paper which is devoted to understand the double effect of surface tension and adding nanoparticles on 3D natural convection.

2. Mathematical model

2.1. Definition of geometrical configuration and assumptions

The three-dimensional natural convective flow inside a cubical enclosure [width = height = (l)] filled with water-Al_2O_3 nanofluid is considered in the present work. The physical model with coordinates is presented in Fig. 1.

The left sidewall of the enclosure is maintained at hot temperature, while the right sidewall is maintained at cold temperature. The other enclosure walls are considered adiabatic. The top surface of the liquid is free and in contact with the gas above. The thermo-physical properties of base fluid (water) and Al_2O_3 nanoparticles are listed in Table 1. The problem is modeled mathematically based on the following assumptions:

(a) The flow is considered Newtonian, three-dimensional, unsteady, laminar and incompressible.
(b) Both the base fluid phase and nanoparticles are assumed to be in thermal equilibrium state.
(c) Both the base fluid and nanoparticles have constant thermo-physical properties and the density variation is modeled using Boussinesq approximation.
(d) Heat generation and viscous dissipation in the fluid are negligible.
(e) No slip occurs between base fluid and nanoparticles.
(f) The nanofluid is assumed to be in a single phase and nanoparticles have uniform sizes and shapes.

In the present work, the Rayleigh number (Ra) is fixed at 10^5, while the solid volume fraction, (φ) and Marangoni number (Ma) have been varied respectively from 0% to 20% and −1000 to 1000. The Prandtl number of water (i.e. base fluid) is taken as (Pr = 6.2).

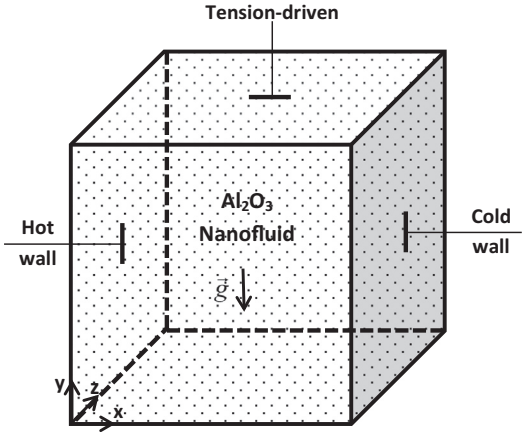

Figure 1 Physical model with coordinates.

Table 1 Thermophysical properties of water and Al_2O_3 nanoparticles.

Physical properties	Water	Al_2O_3
C_p (J/kg K)	4179	765
ρ (kg/m^3)	997.1	3970
k (W/m K)	0.613	40
$\alpha \times 10^7$ (m^2/s)	1.47	131.7
$\beta \times 10^{-5}$ (1/K)	21	0.85

2.2. Governing equations and numerical solution

To solve the considered problem, the vorticity-vector potential formalism ($\vec{\psi} - \vec{\omega}$) is considered which allows in a 3-D configuration, the elimination of the pressure gradient terms. The vector potential and the vorticity are defined respectively by the following two relations:

$$\vec{\omega}' = \vec{\nabla} \times \vec{V}' \text{ and } \vec{V}' = \vec{\nabla} \times \vec{\psi}' \tag{1}$$

The governing equations can be written in non-dimensional forms as follows:

$$-\vec{\omega} = \nabla^2 \vec{\psi} \tag{2}$$

$$\frac{\partial \vec{\omega}}{\partial t} + (\vec{V}.\nabla)\vec{\omega} - (\vec{\omega}\cdot\nabla)\vec{V} = \left[\frac{Pr}{(1-\varphi)^{0.25}\left((1-\varphi)+\varphi\frac{\rho_s}{\rho_f}\right)}\right]\Delta\vec{\omega} + Ra\,Pr\left[\frac{1}{\frac{(1-\varphi)}{\varphi}\frac{\rho_f}{\rho_s}+1}\frac{\beta_s}{\beta_f}+\frac{1}{\frac{\varphi}{(1-\varphi)}\frac{\rho_f}{\rho_s}+1}\right]\left[\frac{\partial T}{\partial z};0;-\frac{\partial T}{\partial x}\right] \tag{3}$$

$$\frac{\partial T}{\partial t} + \vec{V}.\nabla T = \left[\frac{\frac{k_{nf}}{k_f}}{(1-\varphi)+\varphi\frac{(\rho c_p)_s}{(\rho c_p)_f}}\right]\nabla^2 T \tag{4}$$

The time (t'), velocity ($\vec{V}'$), vector potential ($\vec{\psi}'$) and vorticity ($\vec{\omega}'$), are put respectively in their dimensionless forms by l^2/α_f, α_f/l, α_f and l^2/α_f and the non-dimensional temperature is defined by $T = (T' - T'_c)/(T'_h - T'_c)$.

In the above equations, the dimensionless parameters, Prandtl and Rayleigh numbers are defined respectively as

$$Pr = \frac{\nu_f}{\alpha_f} \quad \text{and} \quad Ra = \frac{g.\beta_f \cdot \Delta T.l^3}{\nu_f \cdot \alpha_f} \tag{5}$$

The effect of the Brownian motion of nanoparticles is neglected and the expressions of the thermo-physical properties are given as below:

– The effective density of the nanofluid is given by Kahveci [18] as follows:

$$\rho_{nf} = (1-\varphi)\rho_f + \varphi\rho_s \tag{6}$$

– The heat capacitance of the nanofluid is expressed as Kahveci [17]:

$$(\rho C_p)_{nf} = (1-\varphi)(\rho C_p)_f + \varphi(\rho C_p)_s \tag{7}$$

– The effective thermal conductivity of the nanofluid is approximated by the Maxwell–Garnetts model as follows:

$$\frac{k_{nf}}{k_f}=\frac{k_s+2k_f-2\varphi(k_f-k_s)}{k_s+2k_f+\varphi(k_f-k_s)} \tag{8}$$

– The effective dynamic viscosity of the nanofluid is given by Brinkman [19] asfollows:

$$\mu_{nf}=\frac{\mu_f}{(1-\varphi)^{2.5}} \tag{9}$$

2.3. Boundary conditions

The boundary conditions for the present problem are given as follows:

Temperature:

$$T=1 \text{ at } x=1,\ T=0 \text{ for } x=0 \tag{10}$$

$$\frac{\partial T}{\partial n}=0 \text{ on other walls (adiabatic).} \tag{11}$$

Vorticity:

$$\omega_x=0,\omega_y=-\frac{\partial V_z}{\partial x},\omega_z=\frac{\partial V_y}{\partial x} \text{ at } x=0 \text{ and } 1 \tag{12}$$

$$\omega_x=\frac{\partial V_z}{\partial y},\omega_y=0,\omega_z=-\frac{\partial V_x}{\partial y} \text{ at } y=0 \text{ and } 1 \tag{13}$$

$$\omega_x=-\frac{\partial V_y}{\partial z},\omega_y=\frac{\partial V_x}{\partial z},\omega_z=0 \text{ at } z=0 \text{ and } 1 \tag{14}$$

Vector potential:

$$\frac{\partial \psi_x}{\partial x}=\psi_y=\psi_z=0 \text{ at } x=0 \text{ and } 1 \tag{15}$$

$$\psi_x=\frac{\partial \psi_y}{\partial y}=\psi_z=0 \text{ at } y=0 \text{ and } 1 \tag{16}$$

$$\psi_x=\psi_y=\frac{\partial \psi_z}{\partial z}=0 \text{ at } z=0 \text{ and } 1 \tag{17}$$

Velocity:

$$V_x=V_y=V_z=0 \text{ at } x=0,x=1,z=0,z=1 \text{ and } y=0 \tag{18}$$

$$V_y=0;\frac{\partial V_x}{\partial y}=-Ma\frac{\partial T}{\partial x} \text{ and } \frac{\partial V_y}{\partial y}=-Ma\frac{\partial T}{\partial z} \text{ at } y=1 \text{ (free surface).} \tag{19}$$

where the Marangoni number (Ma) is defined as follows:

$$Ma=\left(\frac{\partial \sigma}{\partial T}\right)\frac{\Delta T}{\alpha_{nf}\mu_{nf}} \tag{20}$$

The generated entropy (S'_{gen}) is written in the following form by Kolsi et al. [20]:

$$S'_{gen}=\left\{\frac{k_{nf}}{T_0^2}\left[\left(\frac{\partial T'}{\partial x'}\right)^2+\left(\frac{\partial T'}{\partial y'}\right)^2+\left(\frac{\partial T'}{\partial z'}\right)^2\right]\right\}+\frac{\mu_{nf}}{T_0}\left\{\begin{array}{l}2\left[\left(\frac{\partial V'_x}{\partial x'}\right)^2+\left(\frac{\partial V'_y}{\partial y'}\right)^2+\left(\frac{\partial V'_z}{\partial z'}\right)^2\right]\\+\left(\frac{\partial V'_y}{\partial x'}+\frac{\partial V'_x}{\partial y'}\right)^2+\left(\frac{\partial V'_z}{\partial y'}+\frac{\partial V'_y}{\partial z'}\right)^2+\left(\frac{\partial V'_x}{\partial z'}+\frac{\partial V'_z}{\partial x'}\right)^2\end{array}\right\} \tag{21}$$

The dimensionless local generated entropy (N_e) is written in the following way:

$$N_e=\frac{k_{nf}}{k_f}\left[\left(\frac{\partial T}{\partial x}\right)^2+\left(\frac{\partial T}{\partial y}\right)^2+\left(\frac{\partial T}{\partial z}\right)^2\right]+\varphi_S\frac{\mu_{nf}}{\mu_f}\left\{\begin{array}{l}2\left[\left(\frac{\partial V_x}{\partial x}\right)^2+\left(\frac{\partial V_y}{\partial y}\right)^2+\left(\frac{\partial V_z}{\partial z}\right)^2\right]\\+\left[\left(\frac{\partial V_y}{\partial x}+\frac{\partial V_x}{\partial y}\right)^2+\left(\frac{\partial V_z}{\partial y}+\frac{\partial V_y}{\partial z}\right)^2+\left(\frac{\partial V_x}{\partial z}+\frac{\partial V_z}{\partial x}\right)^2\right]\end{array}\right\} \tag{22}$$

where $\varphi_e=\left(\frac{\alpha_f}{l\Delta T}\right)^2T_0$ is the irreversibility coefficient.

The first term ($N_{e\text{-}th}$) of the dimensionless local generated entropy represents the local irreversibility due to temperature gradients and the second term ($N_{e\text{-}fric}$) represents the irreversibility due to viscous effects. It is useful to mention that Eq. (22) gives a good idea on the profile and the distribution of the dimensionless local generated entropy (N_e).

The total dimensionless generated entropy (S_{tot}) is written as follows:

$$S_{tot}=\int_v N_e dv=\int_v (N_{e\text{-}th}+N_{e-fr})dv=S_{th}+S_{fr} \tag{23}$$

The Bejan number (Be) is the ratio of heat transfer irreversibility to the total irreversibility:

$$Be=\frac{S_{th}}{S_{th}+S_{fr}} \tag{24}$$

The local Nusselt number (Nu) is defined as follows:

$$Nu=\left(\frac{k_{nf}}{k_f}\right)\left.\frac{\partial T}{\partial x}\right|_{x=0,1} \tag{25}$$

While, the average Nusselt number (Nu_{av}), on the isothermal walls is expressed by the following:

$$Nu_{av}=\int_0^1\int_0^1 Nu.dy.dz \tag{26}$$

The mathematical model described above was written into a FORTRAN program. The control volume method is used to discretize governing Eqs. (2)-(4) and (22). The central-difference scheme is used for treating convective terms while the fully implicit procedure is used to discretize the temporal derivatives. The grids are considered uniform in all directions with additional nodes on boundaries. The successive relaxation iteration scheme is used to solve the resulting nonlinear algebraic equations. The time step (10^{-4}) and spatial mesh (51^3) are utilized to carry out all the numerical tests. The solution is considered acceptable when the following convergence criterion is satisfied for each step of time:

$$\sum_i^{1,2,3}\frac{\max|\psi_i^n-\psi_i^{n-1}|}{\max|\psi_i^n|}+\max|T_i^n-T_i^{n-1}|\leqslant 10^{-5} \tag{27}$$

For the numerical simulation we used an Intel core i7 microprocessor with a 8 Go RAM, the time of execution was about 3 h for $Ra = 10^5$.

The validation of the used program and the justification of the chosen mesh were made in the previous works of Oztop et al. [7] and of Kolsi et al. [17].

Please cite this article in press as: L. Kolsi et al., Numerical investigation of combined buoyancy-thermocapillary convection and entropy generation in 3D cavity filled with Al_2O_3 nanofluid, Alexandria Eng. J. (2016), http://dx.doi.org/10.1016/j.aej.2016.09.005

3. Results and discussion

Thermocapillary effect is a surface tension driven phenomenon and hence it primarily affects the flow near the free surface of the cavity. Natural convection, on the contrary, is caused by temperature gradients present in the body of the fluid and for this reason its effects are distributed in the bulk of the flow field. The results are presented for thermocapillary and buoyancy driven convection of Al_2O_3 nanofluid with volumetric concentration varying from 0% to 20%. The nanoparticles are assumed to be spherical. The bulk temperature variation is low enough for the reliability of Boussinesq approximation in the range of applied Marangoni and Rayleigh numbers. Several numerical test cases have been computed in order to study the various effects of surface tension, buoyancy and nanoparticles concentration on the flow structure of heat transfer and entropy generation. The sign of Marangoni number (Ma) has been chosen in such a way that positive Ma effect increases the buoyancy convection and negative Ma opposes it.

Figs. 2 and 3 present respectively the particle trajectories and projections of velocity vectors in the central x-y plan for different Marangoni numbers and different volumetric concentrations of Al_2O_3 nanoparticles. In opposition with the 2D cases the contours of the streamlines are not closed and particles move from a constant z plan to another. The flow structure is characterized by a central spiralling flow and a ''peripheral'' spiralling flow near the lateral walls. The spiralling flow is divergent (toward the front and back walls) near the lateral walls and convergent toward the x–y central plan in the center.

In the absence of shear at the free surface ($Ma = 0$), the flow exhibits two central vortexes, rising up along the hot wall and sinking along the cold wall of the cavity.

For $Ma = 1000$, thermocapillary effect is added to the buoyancy one causing an intensification of the flow especially near the upper free wall. Compared to the $Ma = 0$ case the flow structure is still constituted by two vortexes. Due to the combination of buoyancy and thermocapillary forces these vortexes are slightly higher.

For $Ma = -1000$, due to the negative value of Marangoni number, there is an opposition of effects between buoyancy and surface tension. The thermocapillary convection causes a downward flow near the free surface while buoyancy driven convection acts in the opposite direction. For this reason, the two different contributions are clearly distinguished and the flow is divided into two regions: the upper one where the motion is induced by surface tension and the lower one driven by buoyancy effects. The Marangoni effect is confined in the upper right corner, with the apparition of a counter-rotating thermocapillary vortex. This vortex is divergent from the central plan toward the front and back walls. The appearance and the position of the central spiralling flow are almost insensitive to the thermocapillary effect but the opposition of the two effects reduces the intensity of the flow.

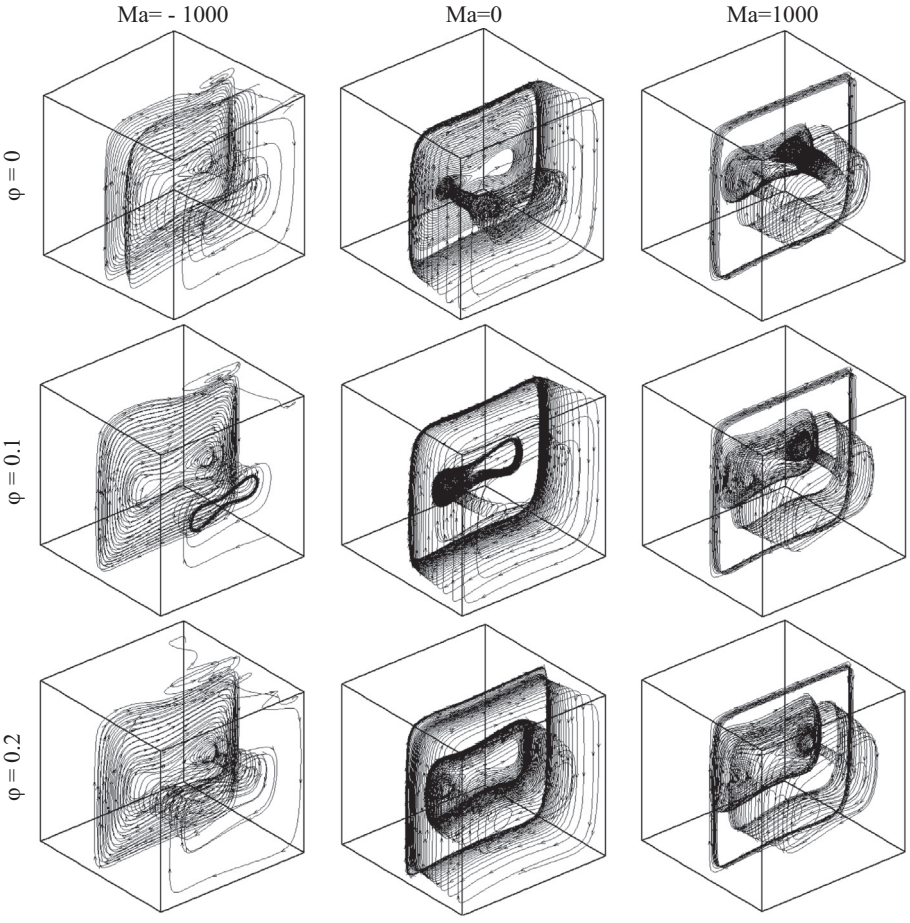

Figure 2 Some Particles trajectories for different Marangoni numbers and different volume fractions of nanoparticles.

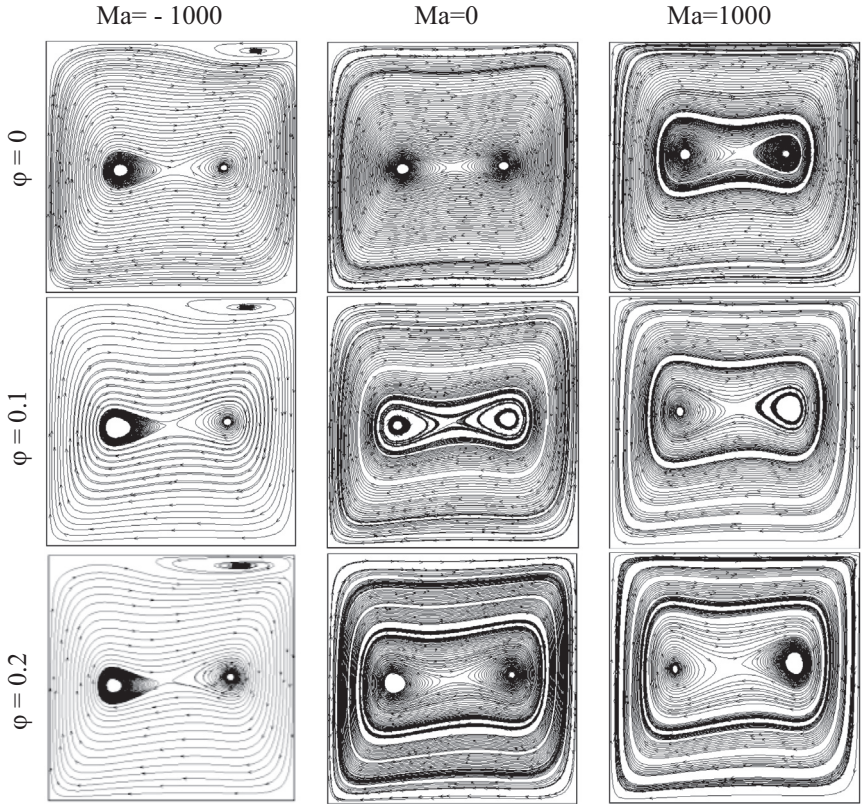

Figure 3 Vector velocity projection in the central *x-y* plan for different Marangoni numbers and different volume fractions of nanoparticles.

For all Marangoni numbers, the flow intensity increases by increasing the nanoparticles volume fraction as a result of high thermal energy transport through the flow related to the high movement of nanoparticles. This flow enhancement is accompanied by an enlargement of the thermal vortexes especially for $Ma = 1000$, and in this case the distance between the vortexes centers increases from 0.398 to 0.472 by increasing the concentration of nanoparticles from 0 to 0.2. For $Ma = -1000$ the size of the thermocapillary vortex increases also by increasing the volume fraction showing that adding nanoparticles enhance both buoyancy and thermocapillary effects.

To evaluate the thermocapillary effect on the three-dimensional flow, the variation of the maximum of the transverse velocity according to Marangoni number is presented in Fig. 4. This figure shows that the thermocapillary effect increases the 3D character of the flow, and this increase is more pronounced for positive Marangoni numbers. The adding of nanoparticles enhances the 3D character of the flow for negative Marangoni numbers and diminishes it for positive numbers.

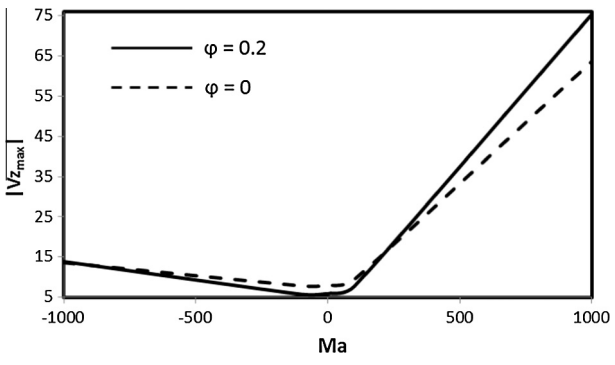

Figure 4 Transverse velocity versus Marangoni number.

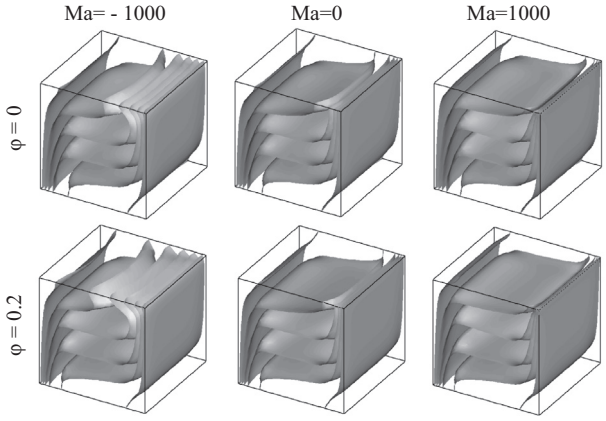

Figure 5 Iso-surfaces of temperature for different Marangoni numbers and different volume fractions of nanoparticles.

Figs. 5 and 6, present respectively the iso-surfaces of temperature and the isotherms in the central *x-y* plan for different Marangoni numbers and different volumetric fractions of

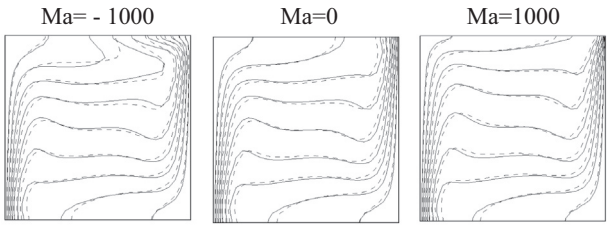

Figure 6 Isotherms in the central *x-y* plan for different Marangoni numbers; $\varphi = 0$ (Dashed) and $\varphi = 0.2$ (Solid).

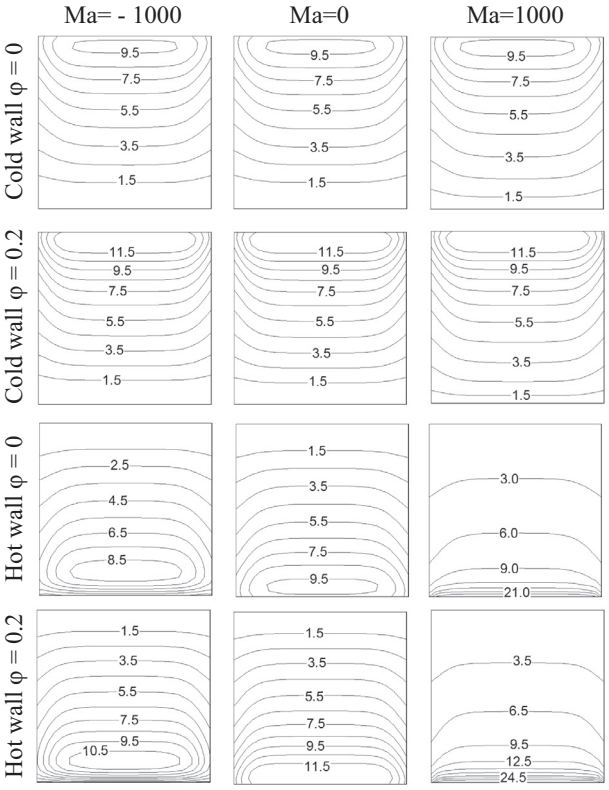

Figure 7 Contours of local Nusselt number at cold and hot walls for different Marangoni numbers and nanoparticles volume fractions.

nanoparticles. For a pure fluid ($\varphi = 0$) and for $Ma = 0$, the isotherms at the center of the cavity are horizontal (vertical stratification) and become vertical only inside the thermal boundary layers at the vertical walls. This vertical stratification breaks down with an increase in the volume fraction of nanoparticles.

For positive $Ma = 1000$ there is a strong thermal boundary layer located close to the upper-right corner due to the cooperative effect of thermocapillary and buoyancy convections in the vicinity of the free surface.

The negative Ma causes a penetration of hot fluid from the upper right corner to the middle of the free surface due to the combined effect of the two counter-rotating recirculations. This penetration leads to the distortion of isotherms near to the upper right corner. By increasing the volume fraction the distortion becomes more intense due to the enlargement of the thermocapillary vortex.

Fig. 7 illustrates the contours of local Nusselt number at hot and cold walls for different Marangoni numbers and different volume fractions. As seen from the figure, the values of the iso-contours of local Nusselt number along hot wall decrease from bottom to top (the reverse is true for the cold wall) but they are almost symmetrically distributed. In the presence of thermocapillary effect, iso-contours of local Nusselt number are concentrated near the bottom of the hot wall especially for positive Marangoni numbers where huge numbers are formed. For negative Marangoni numbers there is a reduction in local Nusselt number at the bottom of the hot wall and an increase at the top. For the cold wall the thermocapillary effect is less influencing and a very light increase occurs at the bottom. By adding nanoparticles an enhancement of the heat transfer is noticed in the entire of the cold and hot walls.

As presented in Fig. 8, by increasing the Marangoni number, Nusselt number increases, and this increase is more important at hot wall than at the cold wall. As expected, in the presence of the thermocapillary and buoyancy driven convection, the Nusselt number is greater for positive values of Marangoni numbers and smaller for negative ones. As expected by increasing the volume fraction, the Nusselt number increases in both cases. It is noticed that for $Ma \approx -330$ there is equilibrium of heat transfers in cold and hot walls.

Contours of local entropy generation due to heat transfer, fluid friction and total entropy generation for $\varphi_s = 10^{-4}$ are presented for different Marangoni numbers and different volume fractions in Fig. 9.

As described before the isotherms are more closely packed near the active walls and in the upper right corner of the cavity (for $Ma = -1000$). In other words, a higher temperature gradient exists in these regions of the cavity, and thus a greater local entropy generation due to heat transfer occurs as a result. In the same way the local entropy generation due to friction is concentrated near to the active walls due to the high upward and downward velocities. For $Ma = -1000$ contours occur also at the upper right corner due to existence of the counter-rotating thermocapillary vortex. The contours of total local entropy generation are almost similar to the contours of entropy due to friction indicating its dominance.

In Figs. 10–12, different forms of entropy generation are shown for the effects of Marangoni number and nanoparticles volume fraction. It should be noted in Fig. 10 that, the entropy generation due to heat transfer increases by increasing volume

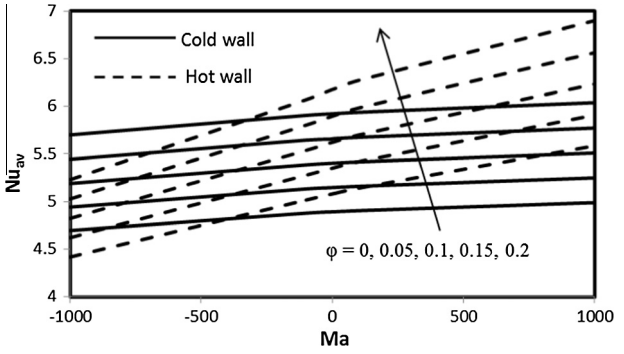

Figure 8 Average Nusselt number versus Marangoni number for different nanoparticles volume fractions.

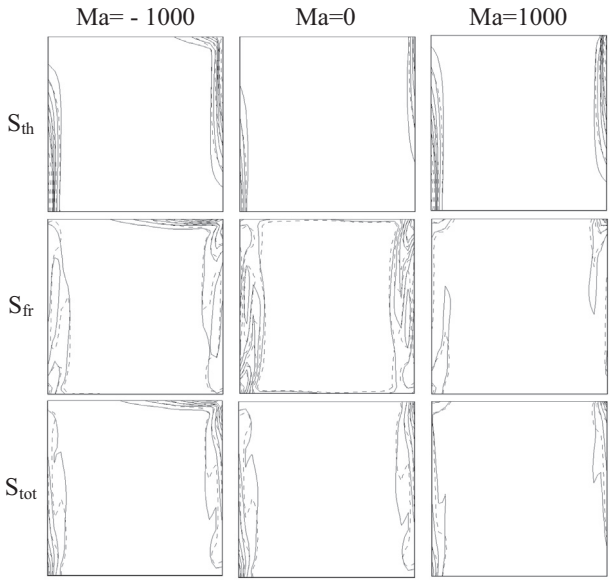

Figure 9 Contours of local entropies generation for $\varphi_s = 10^{-4}$; $\varphi = 0$ (Dashed) and $\varphi = 0.2$ (Solid).

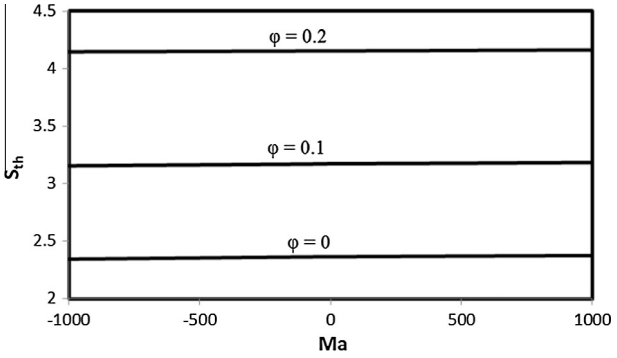

Figure 10 Entropy generation due to heat transfer versus Marangoni number for different nanoparticles volume fractions.

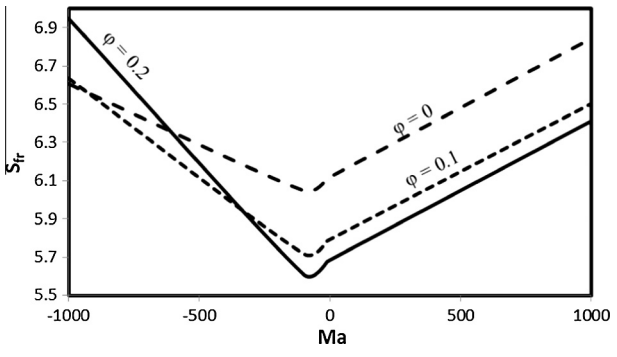

Figure 11 Entropy generation due to friction versus Marangoni number for different nanoparticles volume fractions.

fraction due to the higher temperature gradient and is quasi-constant as function of Marangoni. However, Fig. 11 indicates that the presence of thermocapillary effect increases entropy due to friction. For $Ma > -330$ the increase in volume

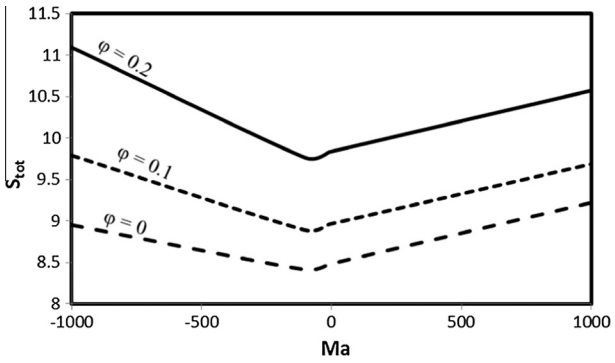

Figure 12 Total entropy generation versus Marangoni number for different nanoparticles volume fractions.

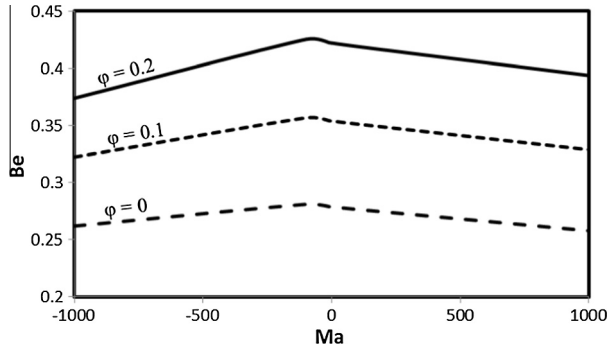

Figure 13 Bejan number versus Marangoni number for different nanoparticles volume fractions.

fraction causes the reduction in entropy generation due to viscous effects. For $Ma < -330$ this variation is decreasing and then increasing. Variation of total entropy generation is shown in Fig. 12. As observed, the thermocapillary effect and adding nanoparticles volume fraction increase the total entropy generation for both negative and positive Marangoni numbers.

Variations of Bejan number with Marangoni number for different volume fractions are presented in Fig. 13. As seen from the figure, Bejan number exhibits almost symmetric behavior according to Marangoni number. The variation is non-monotone with a maximum at $Ma = -10$. For a pure fluid ($\varphi = 0$), variation of Bejan number shows that entropy due to viscous effect is dominant. This dominance reduces significantly by increasing the volume fraction of nanoparticles.

4. Conclusion

In this study a numerical investigation into combined buoyancy and thermocapillary driven convection and entropy generation within a 3D differentially heated enclosure containing Al_2O_3-water nanofluid is performed. In performing the simulations, the governing equations have been modeled using the 3D vorticity-vector potential formalism and then solved using the finite volume method. The simulations have focused specifically on the effects of nanoparticles volume fraction, and Marangoni number on flow structure, isothermal distribution, average Nusselt number and entropy generation within the enclosure.

Please cite this article in press as: L. Kolsi et al., Numerical investigation of combined buoyancy-thermocapillary convection and entropy generation in 3D cavity filled with Al_2O_3 nanofluid, Alexandria Eng. J. (2016), http://dx.doi.org/10.1016/j.aej.2016.09.005

The main important findings can be listed as follows:

- For $Ma > 0$, thermocapillary effect is added to the effect of buoyancy causing an intensification of the flow.
- For $Ma < 0$, the thermocapillary convection causes a downward flow near the free surface while buoyancy driven convection acts in the opposite direction.
- For all Marangoni numbers, the intensity of the flow increases by increasing the solid volume fraction of nanofluid.
- By increasing the Marangoni number, Nusselt number increases. This increase is more important at hot wall than at the cold wall.
- The thermocapillary effect and adding nanoparticles volume fraction increase the total entropy generation for both negative and positive Marangoni numbers.

References

[1] J.C. Maxwell, A Treatise on Electricity and Magnetism, second ed., Oxford University Press, Cambridge, 1904.
[2] J. Straub, J. Betz, R. Marek, Enhancement of heat transfer by thermocapillary convection around bubbles – a numerical study, Numer. Heat Transfer, Part A 25 (1994) 501–518.
[3] M. Behnia, F. Stella, G. Guj, A numerical study of three-dimensional combined buoyancy and thermocapillary convection, Int. J. Multiphase Flow 21 (1995) 529–542.
[4] L. Peng, Y.R. Li, W.Y. Shi, N. Imaishi, Three-dimensional thermocapillary-buoyancy flow of silicone oil in a differentially heated annular pool, Int. J. Heat Mass Transfer 50 (2007) 872–880.
[5] K.J. Lee, Y. Kamotani, S. Yoda, Combined thermocapillary and natural convection in rectangular containers with localized heating, Int. J. Heat Mass Transfer 45 (2002) 302–306.
[6] V. Babu, S.A. Korpela, Three-dimensional thermocapillary convection in a cavity, Comput. Fluids 18 (1990) 229–238.
[7] Hakan F. Oztop, Kolsi Lioua, Borjini Mohamed Naceur, Khaled Al-Salem, Numerical study of three-dimensional combined buoyancy and thermocapillary convection and evaluation of entropy generation, Int. J. Numer. Meth. Heat Fluid Flow 24 (1) (2014) 148–168.
[8] Khalil Khanafer, Kambiz Vafai, Marilyn Lightstone, Buoyancy-driven heat transfer enhancement in a two-dimensional enclosure utilizing nanofluids, Int. J. Heat Mass Transf. 46 (2003) 3639–3653.
[9] Hakan F. Oztop, Eiyad Abu-Nada, Numerical study of natural convection in partially heated rectangular enclosures filled with nanofluids, Int. J. Heat Fluid Flow 29 (2008) 1326–1336.
[10] Amir Houshang Mahmoudi, Mina Shahi, Abbas Honarbakhsh Raouf, Ali Ghasemian, Numerical study of natural convection cooling of horizontal heat source mounted in a square cavity filled with nanofluid, Int. Commun. Heat Mass Transfer 37 (2010) 1135–1141.
[11] Amir Houshang Mahmoudi, Mina Shahi, Abbas Honarbakhsh Raouf, Modeling of conjugated heat transfer in a thick walled enclosure filled with nanofluid, Int. Commun. Heat Mass Transfer 38 (2011) 119–127.
[12] Mostafa Mahmoodi, Numerical simulation of free convection of nanofluid in a square cavity with an inside heater, Int. J. Therm. Sci. 50 (2011) 2161–2175.
[13] Mostafa Mahmoodi, Saeed Mazrouei Sebdani, Natural convection in a square cavity containing a nanofluid and an adiabatic square block at the center, Superlattices Microstruct. 52 (2012) 261–275.
[14] Rehena Nasrin, M.A. Alim, Free convective flow of nanofluid having two nanoparticles inside a complicated cavity, Int. J. Heat Mass Transf. 63 (2013) 191–198.
[15] Hamdy Hassan, Heat transfer of Cu–water nanofluid in an enclosure with a heat sink and discrete heat source, Eur. J. Mech. B/Fluids 45 (2014) 72–83.
[16] Douglas Hector Fontes, Daniel Dall'Onder dos Santos, Elie Luis Martínez Padilla, Enio Pedone Bandarra Filho, Two numerical modelings of free convection heat transfer using nanofluids Inside a Square enclosure, Mech. Res. Commun. 66 (2015) 34–43.
[17] Lioua Kolsi, Ahmed Kadhim Hussein, Mohamed Naceur Borjini, H.A. Mohammed, Habib Ben Aïssia, Computational analysis of three-dimensional unsteady natural convection and entropy generation in a cubical enclosure filled with water-Al_2O_3 nanofluid, Arab. J. Sci. Eng. 39 (2014) 7483–7493.
[18] K. Kahveci, Buoyancy driven heat transfer of nanofluids in a tilted enclosure, ASME J. Heat Transfer 132 (2010) 29–541.
[19] H. Brinkman, The viscosity of concentrated suspensions and solutions, J. Chem. Phys. 20 (1952) 571–581.
[20] L. Kolsi, H. Oztop, M. Borjini, K. Al-Salem, Second law analysis in a three-dimensional lid-driven cavity, Int. Commun. Heat Mass Transfer 38 (2011) 1376–1383.
[21] H. Aminfar, M. Mohammadpourfard, F. Mohseni, Numerical investigation of thermocapillary and buoyancy driven convection of nanofluids in a floating zone, Int. J. Mech. Sci. 65 (2012) 147–156.

Please cite this article in press as: L. Kolsi et al., Numerical investigation of combined buoyancy-thermocapillary convection and entropy generation in 3D cavity filled with Al_2O_3 nanofluid, Alexandria Eng. J. (2016), http://dx.doi.org/10.1016/j.aej.2016.09.005